Volume 21, No 4 | International Journal of Radiation Research, October 2023

# Modification of binomial lateral spreading function for oblique electron beams in pencil beam algorithm based on Monte Carlo simulations

**N. Kholghi[1], M. Pouladian[2*], A. Shabestani Monfared[3]**

*[1]Department of Medical Radiation Engineering, Islamic Azad University, Science and Research Branch, Tehran, Iran*
*[2]Department of Biomedical Engineering, Islamic Azad University, Science and Research Branch, Tehran, Iran*
*[3]Cancer Research Center, Health Research Institute, Babol University of Medical Sciences, Babol, Iran*

► ***Original article***

***Corresponding author:***
*Majid Pouladian, Ph.D.,*
***E-mail:*** *pouladian@srbiau.ac.ir*

**Received:** August 2022
**Final revised:** March 2023
**Accepted:** March 2023

***Int. J. Radiat. Res., October 2023; 21(4): 789-795***

**DOI:** 10.52547/ijrr.21.4.26

***Keywords:*** *Pencil beam, Monte Carlo, oblique beams, binominal gaussian function, lateral spreading parameter.*

## ABSTRACT

***Background***: The present study aimed to evaluate the accuracy of the pencil beam algorithm (PBA) dose calculations with modified binomial lateral spreading function for oblique electron beams compared with Monte Carlo simulations (MCs), as a standard method. ***Materials and Methods***: The oblique pencil beams were simulated using MC code, and lateral dose distributions of oblique (10 and 12 MeV) electron beams were calculated in homogeneous water and heterogeneous slab phantoms (different materials of paraffin, carbon, and RW3). The MC dose calculations were used to modify the parameters of the binomial Gaussian lateral spreading function of PBA. The dose profiles of oblique electron beams were calculated by modified PBA and compared with MCs in both phantoms using gamma analysis with a 2% dose difference (DD) and 2 mm distance to agreement (DTA) constraints. ***Results***: The average difference in dose profiles between PBA and MC calculations was 0.88% and 0.76% for water and slab phantoms, respectively. The mean gamma pass rate was 97.4% and 97.8% for water and slab phantoms, respectively. The gamma pass rates were above 95%, except for the dose profile of the water phantom irradiated with 10 MeV at a depth of 1 cm. ***Conclusion***: The modified PBA dose calculation results showed an excellent agreement with MCs in the two phantoms irradiated with oblique 10 MeV and 12 MeV electron beams. Our approach of modifying the PBA can be used for other charged particle dosimetry and clinical applications, especially electron and proton dosimetry.

## INTRODUCTION

Electron beams (in the energy range of 4-25 MeV) are commonly used in radiation therapy [1]. The electron-delivered dose sharply drops in both lateral and depth directions, which is useful to treat superficial structures such as lymphoma, mycosis fungoides, and neck cancers [2, 3]. In addition, lower doses will deliver to the normal tissues under the skin (up to 6 cm deep) compared to photon irradiation. Electron beams are often irradiated from oblique directions in clinical practice; however, flat phantoms and vertical irradiations are more commonly used for dose verification and calibration [4]. In electron radiotherapy, the applicator end is not parallel to the skin surface, creating non-uniform geometry and oblique direction. This oblique irradiation changes the dose distribution from parallel irradiation. Therefore, oblique beams and their parameters should be reviewed and commissioned in dose calculation algorithms for clinical applications [4].

Although the pencil beam algorithm (PBA) is still widely used in radiotherapy to calculate the dose of charged particles such as electrons and protons [5], the Gaussian pencil beam electron algorithm based on Fermi-Eyges multiple scattering theory and considered as a non-statistical approach, does not correspond with the measured data [6]. The standard and accurate dosimetry method for simulating the dose distribution in radiotherapy is Monte Carlo simulation (MCs), which has been developing in scientific software packages such as MC N-Particular (MCNP) [7], EGSnrc [8], PRIMO [9], PENELOPE [10], and GATE [11]. Several investigations utilized the MCs available in commercial treatment planning systems; however, their dose calculation procedures are usually time-consuming [12–15].

Shimozato and Okudaira [16] calculated dose distribution using beam data for a typical tube by two MC and generalized Gaussian PBA. The calculated and measured data were evaluated based on dose and depth difference. In their evaluation, two different types of electron irradiation, i.e., oblique angles of 45° and vertical irradiation (angles of 0°), were used. There was a good agreement between the MC and

PBA dose calculations for vertical electron irradiations; however, a poor agreement was found between MC and PBA calculations for oblique angles of 45° in higher depths (>5cm). In another study, Haung *et al.* [15] used MCs and a Ray Station treatment planning system with the PBA electron dosimetry algorithm to calculate electron beam [6, 9, 12] and 15 MeV) dose distributions at several geometries. The MC algorithm was tested in the presence of irregular surface contours (curved cylindrical phantom and triangular nasal phantom), and heterogeneities (cork and cortical bone). They reported that there is a poor agreement between the dose distributions of PBA calculations and MCs in the depths below the heterogeneities and irregular surfaces, showing the inaccuracy of conventional PBA calculations for electron dosimetry.

Millions to billions of simulation histories are needed in radiotherapy treatment planning to obtain accurate dose distributions. Therefore, faster dose calculation algorithms like model-based algorithms (pencil beam, collapse cone convolution, and analytical anisotropic algorithm) with appropriate dose calculation accuracy should be used in clinical practice. Although there are some scientific reports in the field of electron beam dosimetry with a PBA, the conventional lateral spreading function suffers from computational errors, especially in higher depths. PBA is a fast dose calculation algorithm, but it needs some modifications in various geometries and boundaries between different materials [16]. Although there are several studies that tried to modify the lateral spreading function for vertical electron irradiation in pencil beam dose calculation algorithm [15, 17], there is no study reporting these modifications for oblique electron irradiations. These modifications must be considered to have an accurate estimation of the absorbed dose in various geometries of irradiation. Therefore, the current study aimed to modify the PBA lateral spreading function parameters using the results of MCs and evaluate modified PBA dose calculation results in comparison with the results of MCs for oblique electron irradiations. The MCs were considered a gold standard dosimetry method. In this regard, dose profiles calculated by modified PBA in selected depths of water and slab phantoms were compared with MC results.

## MATERIALS AND METHODS

### *Phantoms*

In the present study, two phantoms including a rectangular water tank with dimensions of 20×20×20 $cm^3$ (figure 1 a) and a non-homogeneous slab phantom (figure 1 b) were simulated in both MCs and PBA written in MATLAB software. The slab phantom consisted of three cubic slabs of different materials. The materials were: paraffin (2 cm), with a density of 0.93 $gr/cm^3$ close to the lung wall and adipose tissue; activated carbon (5 cm), with a density of 0.39 $gr/cm^3$, close to the tissues involving air gaps; and RW3 (PTW Company, Germany) with a thickness and density of 10 cm and 1.05 $gr/cm^3$, respectively, mimicking the muscles tissue. All the slabs have an area size of 20×20 $cm^2$.

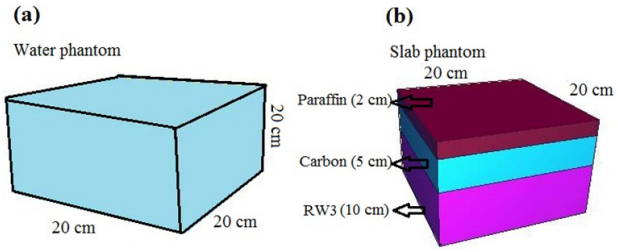


**Figure 1.** The voxelized phantoms used for dose calculation in Monte Carlo simulations and Pencil Beam calculation model. **(a)** water phantom, and **(b)** slab phantom.

### *Monte Carlo simulation*

The geometry of water and slab (heterogeneous) phantoms were defined in the MCNP code (MCNPX 2.6.0 Extensions. Los Alamos National Laboratory, Los Alamos, NM, USA). Oblique (30°) electron pencil beams were simulated in the MC code, and the delivered dose by the electrons was calculated in each voxel. The incident electron beams were considered single-energy electron irradiation with 10 and 12 MeV energies. These irradiations were not produced by an accelerator or a radioactive source, and they just were theoretical single-energy electron radiations to use as a source in our study. Dosimetry voxels were defined in homogeneous and heterogeneous phantoms with the dimensions of 0.2×0.2×0.1 $cm^3$. The cut-off energies were set to 10 keV for photons and electrons. Other simulation parameters including the interactions and cross-sections of electrons and photons were not altered and set to the default settings of the MCNPX program [17]. The particle history was assumed to be equal to $2\times10^8$ for all of the simulations, and the resulting simulation uncertainties were lower than 2%. A splitting factor of 20 was chosen as a variance reduction method. All the simulations were executed on a desktop computer with a 2.6 GHz, 32-core processor and 32 GB of RAM. A square electron applicator was defined at a distance of 5 cm from the surface of the phantom. The source-to-surface distance (SSD) and field size were chosen 100 cm and 14×14 $cm^2$, respectively, for all of the simulations.

### *Pencil beam calculation and modification of PBA lateral spreading function*

The dose profile values in the y direction (direction of oblique beams) were obtained and plotted at different depths (certain distances from the phantom surface) from MCs. The best-fitted binomial Gaussian function for these points was calculated in

MATLAB software. The lateral spreading parameters were found by comparing the best-fitted function with the relevant binomial Gaussian function of PBA. The accuracy of the PBA dose was evaluated based on the MCs (as a gold standard method).

A PBA code was developed and the lateral scattering parameters as a mathematical function based on the results of phantom MCs were imported into an in-house MATLAB program (v.2017b, MathWorks Company, USA). At first, MCs were performed for both phantoms, and then, the PBA calculations were performed on these phantoms and lateral spreading functions of PBA were corrected using the obtained MC results.

The mentioned homogeneous and non-homogeneous slab phantoms were considered and defined in PBA MATLAB code. Similar to MCs, single energy oblique electron irradiations (10 and 12 MeV energies) were defined in PBA calculations. The dose distributions were calculated in the phantoms in the voxels of 0.2×0.2×0.1 $cm^3$ using PBA. The dose resulting from the Bremsstrahlung photons was discarded. Each pencil beam was also simulated by MC to obtain the lateral spreading values. The pencil beam was a flux of single-energy electrons passing through a small section of 0.2×0.2 $cm^2$ at the phantom surface. Each pencil beam has a central axis where electrons diverge at a slight angle. The lateral energy distribution of each pencil beam at a certain depth of a phantom follows a Gaussian function [18].

The dose distributions were also obtained from MCs and were used to obtain the parameters of the lateral spreading Gaussian function (c or σ). In most PBAs, the lateral spreading Gaussian parameter (σ) value is projected using the multiple scattering theory of small Fermi angles [18]. A limitation of this method leads to the unlimited increase of σ with depth, which is contrary to practical measurements. In some research, few corrections were used to modify the lateral spreading of the oblique beams [19]; however, they did not use MC calculations to find the lateral spreading functions of the oblique beams.

In oblique radiations, an angle with the vector perpendicular to the surface creates changes to the Gaussian distribution of the electrons' delivered dose. In this research, the beam angle was considered 30° from the Z-axis direction (the vector perpendicular to the phantom surface). Energy distribution of oblique beams in PBA follows binominal Gaussian functions as Equation 1 [18]:

$$f(z) = a_1 * exp^{-(\frac{x-b_1}{c_1})^2} + a_2 * exp^{-(\frac{x-b_2}{c_2})^2} \quad (1)$$

Where;

$$a_1 = \frac{1}{2\pi c_1^2},\ a_2 = \frac{1}{2\pi c_2^2}$$

Where; $b_1$ and $b_2$ are the distances from the central axis in the x, and y directions. z is the depth from the phantom surface. $c_1$ and $c_2$ are the lateral spreading values calculated from fitting the formula to the lateral dose distribution obtained from MCs. The diagrams in figure 2 show the dose distribution of perpendicular and oblique electron irradiations.

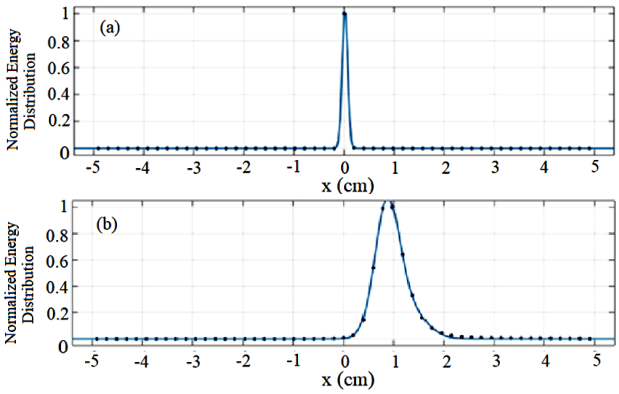


**Table 2.** Statistical data of the radiographic parameters (kVp and mAs values) and patient anthropometric data for selected X-ray examinations.

$$D(x,y,z) = \sum_{k=1}^{n_x}\sum_{l=1}^{n_y} w(x,y) \times \frac{1}{2}\{erf\left[\frac{x_k+\frac{\Delta x}{2}-x}{\sqrt{2}\partial x(x,y,z)}\right] - erf\left[\frac{x_k-\frac{\Delta x}{2}-x}{\sqrt{2}\partial x(x,y,z)}\right]\} \times \frac{1}{2}\{erf\left[\frac{y_l+\frac{\Delta y}{2}-y}{\sqrt{2}\partial_{y1}(x,y,z)}\right] - erf\left[\frac{y_l-\frac{\Delta y}{2}-y}{\sqrt{2}\partial_{y1}(x,y,z)}\right] + \mathrm{erf}\left[\frac{y_l+\frac{\Delta y}{2}-y}{\sqrt{2}\partial_{y2}(x,y,z)}\right] - \mathrm{erf}\left[\frac{y_l-\frac{\Delta y}{2}-y}{\sqrt{2}\partial_{y2}(x,y,z)}\right]\} \times \left[\left[D_{enpt}^{ssE}(z)_{water}^{2a,2b}\right]\right]_p \times erf[\frac{a}{2\sqrt{2}\partial(z)}]^{-1} \times erf[\frac{b}{2\sqrt{2}\partial(z)}]^{-1} \quad (2)$$

The radiation field was reduced into small pixels (Δx × Δy). The size of each pixel was chosen as 0.2×0.2 $cm^2$. $x_k$ and $y_l$ represent the coordinates of each pixel at the z depth. ∂(x, y, z) Refers to the lateral scattering of the pencil beam at point (x, y, z). $(D_{enpt}\ (z))^{a,\ b}{}_{water}$ is the value of the central axis dose along the z-axis for a field of a×b dimensions. W (x, y) is the weight density of beam distribution in the air. $\partial_{y1}$ and $\partial_{y2}$ are the lateral spreading parameters of the oblique beam at the (x, y, z) point along the y-axis. $n_x$ and $n_y$ are the number of networks in the x and y directions, in that order, calculated using equation 3 [19]:

$$N_x = \frac{2a}{\Delta x}, N_y = \frac{2a}{\Delta y} \quad (3)$$

The central axis dose depends on the size of the radiation field; therefore, a correction factor was used for a field of 2a×2b dimensions in all cases [19] (equation 4):

$$\mathrm{erf}[\frac{a}{2\sqrt{2}\partial(z)}]^{-1} \times \mathrm{erf}[\frac{b}{2\sqrt{2}\partial(z)}]^{-1} \quad (4)$$

Similar to MCs, the SSD was chosen 100 cm, and the size of the radiation field was 14×14 $cm^2$. Each pencil beam was simulated from the source, with the beams diverging in the air entering into the dose

calculation volume.

When the applicator end was not parallel to the phantom surface, an inverse-square law of distance was used to correct the dose received in different regions. Oblique beams have differences from direct beams in the air and phantom. Thus, the inverse-square law of distance was used to correct this issue based on equation 5 [19].

$$D(f_{ij},r_{ij}) = (D_{enpt}(z))^{a,b}_{water}\left[\frac{f_{ij}+r_{ij}}{f_0+z}\right]^2 \quad (5)$$

Where $f_0$ is the vertical distance of the virtual source to the vertical phantom surface or the same as SSD, z is the depth in the phantom, $f_{ij}$ is the oblique distance of the virtual source to the $i,j^{th}$ pixel at the phantom surface where the pencil beam passes, and $r_{ij}$ is the route length where the pencil beam travels the phantom as shown in figure 3. The relation between $f_{ij}$, $r_{ij}$, $f_0$, and z was expressed by equations 6 and 7 [18]:

$$f_i = \sqrt{f_0^2 + y_i^2} \quad (6)$$

Where $y_i$ is the horizontal distance of the source to the $i,j^{th}$ pixel at the phantom surface.

$$\frac{f_0}{z} = \frac{f_{ij}}{r_{ij}} \quad (7)$$

If the beam passes through the phantom, $Z_{eff}$ must be used, which is calculated using equation 8 (18).

$$z_{eff}(z) = \int_{\sigma}^{z} \frac{S_m(x_i,y_i,z)}{S_w(x_i,y_i,z)} d\,z \quad (8)$$

$S_m$ ($x_i$, $y_i$) is the stopping power in the phantom matter at $x_i,y_i$ point and $S_w$ ($x_i$, $y_i$) is the stopping power in the water at $x_i,y_i$ point.

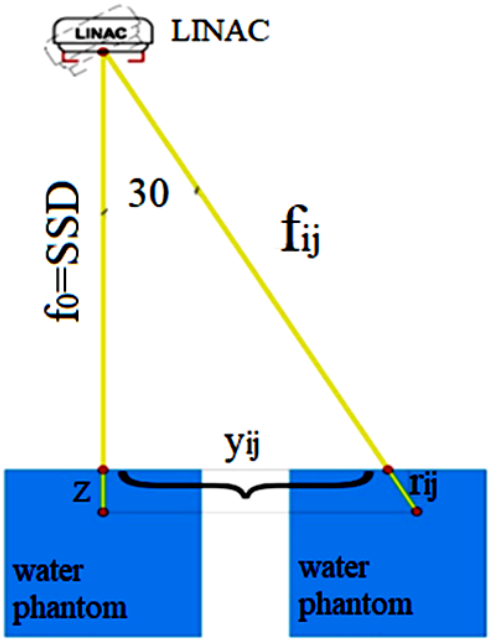


**Figure 3.** Geometry of perpendicular (left) oblique (right) electron beam irradiating to the water phantom.

***Analysis***

The dose profiles of MCs and PBA calculations were obtained and compared by gamma analysis. MC results were considered as reference dose values, and dose values obtained from PBA were considered as calculations. The dose difference (DD) and distance to agreement (DTA) criteria for gamma analysis were chosen as 2% and 2 mm, respectively. The dose threshold for gamma values was 10% of the maximum dose [19].

## RESULTS

The MCs showed that if the central axis of a pencil beam is not perpendicular to the phantom surface, the energy distribution can be estimated as symmetrical which can be calculated using the monomial Gaussian function in surface areas. However, in higher depths, the energy distribution of the oblique pencil beam is no longer symmetrical and must be calculated using a binomial Gaussian function.

The profiles obtained by the PBA and MC calculations for 10 and 12 MeV electron energies along the y-axis at several depths in the homogeneous water phantom are presented in figures 4 and 5. Figure 4 shows the dose profiles at 0.5, 1.1, 2.3, and 3.3 cm depths, for the 12 MeV energy. Figure 5 illustrates the profiles for 10 MeV energy at 0.5, 1, 1.7, and 2.7 cm depths. There is a good agreement between PBA and MC calculations in all the assessed depths and electron energies. In a way that, the mean difference between PBA and MC was lower than 0.4%, and the maximum difference was less than 1.5% occurring in the fields' edge at lower depth (0.5 cm) for both of the electron energies.

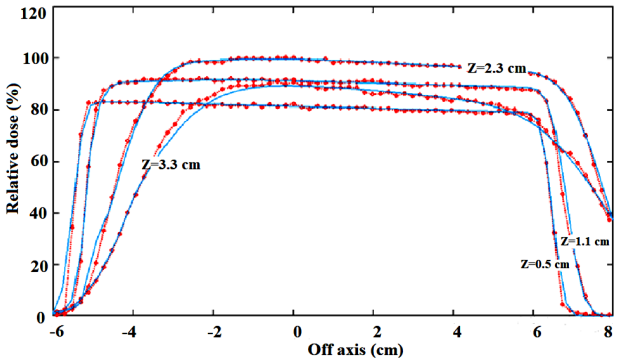


**Figure 4.** Oblique 12 MeV electron beam profiles at 0.5 cm, 1.1 cm, 2.3 cm, and 3.3 cm depths in the water phantom; the dotted lines are related to Monte Carlo simulations while solid lines are related to PBA calculations.

Figure 6 shows the dose profiles obtained from PBA and MC calculations at 1, 1.5, 2.1, and 2.5 cm depths for 12 MeV electron energy in the slab phantom. In addition, for this phantom, the dose profiles for 10 MeV electron energy at 0.5, 1, 1.8, and 2.5 cm depths are illustrated in Figure 7. In the

assessed depths and electron energies, there is a good agreement between PBA and MC calculations. The mean and maximum differences between PBA and MC were lower than 0.9%, and 2.6% (of maximum dose in each profile), respectively, occurring in the fields' edge at lower depth (0.5 cm) and in the depth of boundaries between two different materials. The profiles up to the 2 cm depth are related to the paraffin area, and the 2.1 cm depth is the boundary line between the carbon and paraffin layers.

For the two investigated energies, the maximum dose values in y direction occur in -y direction, due to the oblique irradiation, in the fields' edge regions near the source. The dose value gradually decreases as it turns away from the source and approaches to the positive y direction. The difference between maximum and minimum values along the y direction increased with increasing depth.

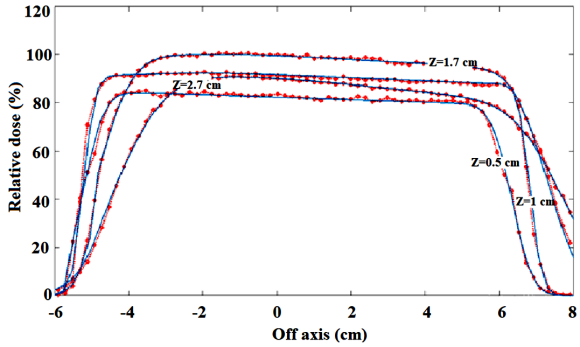


**Figure 5.** Oblique 10 MeV electron beam profiles at 0.5 cm, 1.0 cm, 1.7 cm, and 2.7 cm depths in the water phantom; the dotted lines are related to Monte Carlo simulations while solid lines are related to PBA calculations.

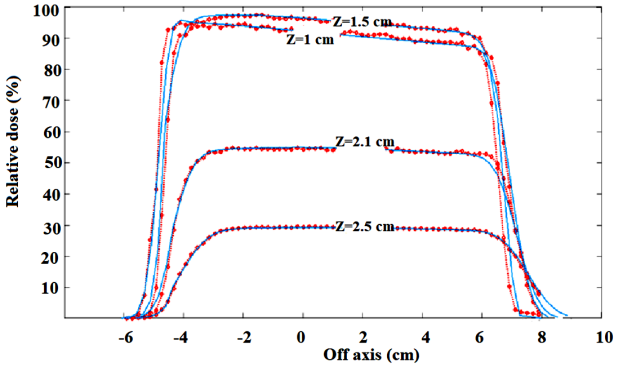


**Figure 6.** Oblique 12 MeV electron beam profiles at 1.0 cm, 1.5 cm, 2.1 cm, and 2.5 cm depths in the slab phantom; the dotted lines are related to Monte Carlo simulations while solid lines are related to PBA calculations.

The mean percentage of differences and gamma pass rate (the percentage of gamma values lower than 1) results of comparing dose profiles obtained by MCs and PBA calculations for oblique 12 and 10 MeV electron irradiation on the water and slab phantoms at the depths of 0.5, 1.1, 2.3, and 3.3 cm are depicted in Table 1. Considering the gamma analysis criteria (2% DD and 2mm DTA), all the pass rates were higher than 95.5% showing very good agreement between MC and PBA calculations, except for dose profiles of 10 MeV irradiation in the depth of 1 cm, which was 94.8 %.

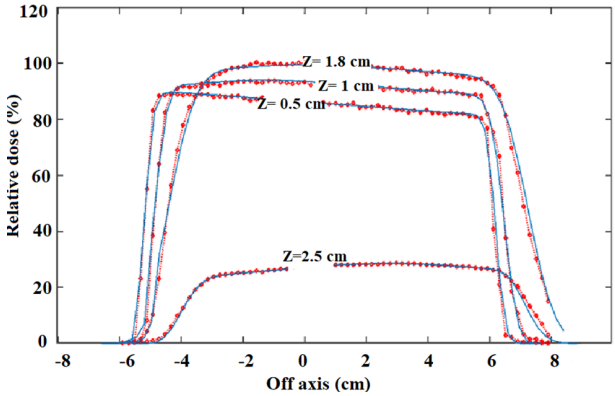


**Figure 7.** Oblique 10 MeV electron beam profiles at 0.5 cm, 1.0 cm, 1.8 cm, and 2.5 cm depths in the slab phantom; the dotted lines are related to Monte Carlo simulations while solid lines are related to PBA calculations.

**Table 1.** The results of the calculated relative dose, mean percentage of the difference between PBA and MC calculations, and gamma index pass rate between PBA and MC dose profiles for the homogeneous water and non-homogeneous slab phantoms irradiated by 10 and 12MeV oblique electron beams.

| Energy (MeV) | Depth (cm) | Max relative dose% (PBA) | Mean percentage of difference (%) | Gamma pass rate (%) |
|---|---|---|---|---|
| **Water phantom** | | | | |
| 12 | 0.54 | 82 | 1.29 | 98.6 |
| 12 | 1.1 | 92 | 0.45 | 100 |
| 12 | 2.3 | 100 | 0.35 | 97.2 |
| 12 | 3.3 | 90 | 1.3 | 97.2 |
| 10 | 0.5 | 84 | 1.1 | 95.8 |
| 10 | 1.0 | 92 | 1.03 | 94.8 |
| 10 | 1.7 | 100 | 0.54 | 98.6 |
| 10 | 2.7 | 90 | 1.01 | 97.2 |
| **Slab phantom** | | | | |
| 12 | 1 | 95 | 0.45 | 98.1 |
| 12 | 1.5 | 98 | 0.355 | 98.5 |
| 12 | 2.1 | 55 | 1.2 | 96.8 |
| 12 | 2.5 | 28.5 | 1.1 | 95.1 |
| 10 | 0.5 | 95 | 0.733 | 98.6 |
| 10 | 1.0 | 98 | 0.83 | 98.1 |
| 10 | 1.8 | 100 | 0.89 | 97.6 |
| 10 | 2.5 | 27 | 0.56 | 100 |

## DISCUSSION

PBA is one of the useful algorithms utilized to estimate the electron beam dose distributions in patients/phantoms; however, the estimated dose can have uncertainties, especially in inhomogeneous regions or irregular irradiation/patient geometries [21, 22]. The lateral spreading monomial or binomial Gaussian function in the PBA losses its accuracy for oblique surfaces or oblique beams. Because the Gaussian function for an oblique pencil beam could be asymmetrical, which is considerable in higher depths [18]. Therefore, we tried to resolve this

problem by modifying the lateral spreading function from the parameters obtained using the MCs. The dose calculation errors for the materials of different densities in relation to the water can be higher, in this regard, we defined heterogeneous slab phantom in MATLAB-based PBA code and MCs to obtain the lateral dose spreading parameters with the use of MCs. Following our findings, the lateral spreading function dose calculation errors were reduced using lateral spreading functions obtained by MCs.

Ding *et al.* [21] assessed the accuracy of PBA dose calculations compared to MCs and measurements. They reported that the accuracy of the conventional PBA calculations depends on the inhomogeneity geometry and location. PBA showed some serious limitations in the prediction of hot and cold regions in heterogeneous phantoms for low or high-density inhomogeneity, particularly for low-energy electron beams (like 9 MeV). Errors (>10%) were found in the prediction of high- and low-dose variations for three-dimensional inhomogeneous phantoms. They also performed a comparison for the oblique incident (for 9 and 20 MeV electron beams) between PBA and measurements in a uniform water phantom [21]. The SSD was 110 cm and the gantry angle was 30°. There was an excellent agreement between calculated and measured data; however, a high discrepancy around 10%, was reported between PBA and measurements in off-axis and oblique irradiation on a heterogeneous lung phantom.

Krieger and Sauer [23] evaluated the accuracy of photon dose calculations of PBA, collapsed cone (CC), and MC algorithms in heterogeneous multi-layer phantom composed of Styrofoam and white polystyrene. The beam axis (6 MV photons with 10*10 and 20*20 field sizes) was aligned parallel to the layers and various field offsets were applied. They found that MC and CC calculations agreed with the measurements whereas the PB algorithm calculated 12% higher doses on average. Furthermore, in off-axis dose profiles, the reported differences between the algorithms increased dramatically. Their results showed that the PB algorithm produces large dose calculation errors in interfaces and low-density regions.

In our study, a good agreement was found between the modified PBA and MC in the water and heterogeneous slab phantoms with oblique electron beams. In line with the current study, Samuelsson *et al.* [24] reported that there is a reasonable agreement between conventional PBA and measurements in oblique electron irradiation on a water phantom.

Chi *et al.* [19] investigated the possibility of modeling electron arc treatment beams using the pencil beam redefinition algorithm (PBRA) with small angular steps. They used the internal heterogeneities of a cylindrical phantom, and reported that PBRA calculated central-axis depth doses agreed with measured doses (2% and 1 mm in the low-dose and high-dose gradient regions, respectively). In addition, the off-axis doses were matched within 3% in the low-dose gradient region and within 2 mm in the high-dose gradient region. They expressed that their PBRA dose calculation model is adequate and accurate for planning electron arc therapy. The conventional PBA was modified in their study by incorporating two correction factors; one for energy, SSD, and field width, and another for large-angle scattering, allowing more accurate calculation of mid-arc dose delivery. Their results were comparable to our findings. We determined that PBA has sufficient accuracy for electron dose calculations in the two phantoms; however, we used MCs for modifying the lateral spreading function of PBA.

Ulmer and Harder [25] represented the transverse profiles of PBA by Triple Gaussian functions for high energy photon beam (Co-60 gamma rays, 6 MV, 8 MV, and 18 MV X-rays) dose calculations. Similar to our approach, they used the MC-generated transverse profiles of photon pencil beams to obtain a lateral scattering function as a sum of three Gaussian functions, whose coefficients and parameters were optimized using the Fourier transform method. They compared the dose distribution resulting from the modified photon PBA and dose measurements in a water phantom. They achieved excellent agreement between PBA calculations and measurements. However, they have not evaluated the effects of oblique photon beams or heterogeneities.

A gamma pass rate of over 95% is routinely accepted in clinical practice for comparing electron dose between two different measurements or calculation methods [25]. Owing to the results, most obtained gammas rates were above 95%, except for dose profiles of 10 MeV irradiation in the depth of 1 cm. Generally, there were good consistencies in all dose profiles obtained by MC and modified-PBA calculations; though, little differences in the fields' edge regions were determined. In agreement with the present work, a previous investigation [17] expressed that the differences in the fields' edge regions could be related to the inherent inaccuracy of dose calculation models (the regions with high dose gradients).

In the current work, oblique beams in homogeneous and heterogeneous phantoms were simulated. However, all the actual materials and geometries in clinical conditions were not covered. Furthermore, there are various oblique fields with different gantry angles and field sizes that can be appropriate subjects for future studies.

## CONCLUSION

We modified the conventional PBA binomial Gaussian function parameters for the lateral

spreading of dose distribution based on the MCs for oblique electron irradiations. The gamma analysis showed that the modified PBA dose calculation findings had excellent agreements with MCs results in homogeneous and heterogeneous phantoms irradiated by oblique 10 and 12 MeV electron beams. Our approach for modifying PBA can be used for other charge particle dose calculations, and clinical applications, especially electron and proton beam dosimetry.

**ACKNOWLEDGMENTS**

*We like to express our appreciation to the SRBIAU (Science and Research Branch, Islamic Azad University) for their cooperation in our study.*

***Conflicts of interest*:** The authors declare no conflict of interest.

***Ethics consideration*:** This work was a simulation study which did not consider any patient or biological material/data.

***Funding*:** No financial support was received from any organization in this study.

***Author contribution*:** MP was responsible for the study conception, design, acquisition of data, and finalizing of the manuscript. All the authors contributed to data analyzing and writing the manuscript draft. Furthermore, all the authors read and approved the final manuscript.

## REFERENCES

1. Jong WL, Ung NM, Tiong AH, *et al.* (2018) Characterisation of a MOSFET-based detector for dose measurement under megavoltage electron beam radiotherapy. *Radiat Phys Chem,* ***144****: 76-84*.
2. Kokurewicz K, Brunetti E, Curcio A, *et al.* (2021) An experimental study of focused very high energy electron beams for radiotherapy. *Commun Phys,* ***4****(1): 1-7*.
3. Labuś W, Kitala D, Klama-Bary\la A, *et al.* (2022) Influence of electron beam irradiation on extracellular matrix of the human allogeneic skin grafts. *J Biomed Mater Res B Appl Biomater,* ***110****(3): 547-563*.
4. Soejoko DS and Adi RW (2007) The influence of oblique incidence electron beams to beam specification parameters. *World Congress on Medical Physics and Biomedical Engineering 2006, p. 1948-1951*.
5. Chamberland E, Beaulieu L, Lachance B (2015) Evaluation of an electron Monte Carlo dose calculation algorithm for treatment planning. *J Appl Clin Med Phys,* ***16****(3): 60-79*.

Hollmark M, Gudowska I, Belkić D, *et al.* (2008) An analytical model for light ion pencil beam dose distributions: multiple scattering of primary and secondary ions. *Phys Med Biol,* ***53****(13): 3477-3491*.

7. Brown FB, Barrett RF, Booth TE, *et al.* (2002) MCNP version 5. *Trans Am Nucl Soc,* ***87****(273): 02-3935*.
8. Kawrakow I and Rogers DWO (2000) The EGSnrc code system. NRC Rep PIRS-701 NRC Ott. 17.
9. Rodriguez M, Sempau J, Brualla L (2013) PRIMO: A graphical environment for the Monte Carlo simulation of Varian and Elekta linacs. *Strahlentherapie und Onkologie,* ***189****(10): 881-6*.
10. Sempau J, Badal A, Brualla L (2011) A PENELOPE-based system for the automated Monte Carlo simulation of clinacs and voxelized geometries—application to far-from-axis fields. *Med Phys,* ***38****(11): 5887-5895*.
11. Şahmaran T and Kaşkaş A (2022) Comparisons of various water-equivalent materials with water phantom using the Geant4/GATE simulation program. *Int J Radiat Res,* ***20****(3): 709-714*.
12. Egashira Y, Nishio T, Hotta K, *et al.* (2013) Application of the pencil-beam redefinition algorithm in heterogeneous media for proton beam therapy. *Phys Med Biol,* ***58****(4): 1169-84*.
13. Zhang H, Li Q, Liu X, *et al.* (2022) Validation and testing of a novel pencil-beam model derived from Monte Carlo simulations in carbon-ion treatment planning for different scenarios. *Phys Med,* ***99****: 1-9*.
14. Al Hassan M, Liu WB, Wang J, *et al.* (2011) Monte Carlo simulations of gamma-rays shielding with phthalonitrile-tungsten borides composites. *Int J Radiat Res,* ***20****(3): 621-626*.
15. Huang JY, Dunkerley D, Smilowitz JB (2019) Evaluation of a commercial Monte Carlo dose calculation algorithm for electron treatment planning. *J Appl Clin Med Phys,* ***20****(6): 184-193*.
16. Shimozato T and Okudaira K (2017) Dose distributions in simulated electron radiotherapy with intraoral cones using treatment planning system. *Int J Med Phys Clin Eng Radiat Oncol,* ***6****(03): 280-289*.
17. Kholghi N, Pouladian M, Monfared AS (2022) Evaluating the accuracy of electron pencil beam dosimetry based on Monte Carlo simulations using homogeneous and heterogeneous phantoms. *Inform Med Unlocked,* ***31****:101006*.
18. Hogstrom KR, Mills MD, Almond PR (1981) Electron beam dose calculations. *Phys Med Biol,* ***26****(3): 445-59*.
19. Chi PCM, Hogstrom KR, Starkschall G, *et al.* (2006) Application of the electron pencil beam redefinition algorithm to electron arc therapy. *Med Phys,* ***33****(7-1): 2369–2383*.
20. Khan FM, Sperduto PW, Gibbons JP (2021) Khan's treatment planning in radiation oncology: Lippincott Williams & Wilkins.
21. Ding GX, Cygler JE, Christine WY, *et al.* (2005) A comparison of electron beam dose calculation accuracy between treatment planning systems using either a pencil beam or a Monte Carlo algorithm. *Int J Radiat Oncol Biol Phys,* ***63****(2): 622–633*.
22. dos Reis Gonçalves F, Vianello E, Viegas C, Viamonte A (2020) Dosimetric evaluation of electron beam Monte Carlo isodoses distribution based on thermoluminescent dosimetry. *Braz J Radiat Sci,* ***8****(1): 1-18*.
23. Krieger T and Sauer OA (2005) Monte Carlo-versus pencil-beam-/collapsed-cone-dose calculation in a heterogeneous multi-layer phantom. *Phys Med Biol,* ***50****(5): 859-868*.
24. Samuelsson A, Hyödynmaa S, Johansson KA (1998) Dose accuracy check of the 3D electron beam algorithm in a treatment planning system. *Phys Med Biol,* ***43****(6): 1529*.
25. Ulmer W and Harder D (2005) A triple Gaussian pencil beam model for photon beam treatment planning. Z *Für Med Phys,* ***5****(1): 25-30*.
26. Klein EE, Hanley J, Bayouth J, *et al.* (2009) Task Group 142 report: Quality assurance of medical accelerators a. *Med Phys,* ***36****(9-1): 4197-4212*.